The Effect of ECAP on Structural Morphology and Wear Behaviour of 5083 Al Composite Reinforced with Red Mud

Brahmananda Reddy Sathi
Department of Mechanical Engineering, JNTUK-UCE : Research Scholar

Swami Naidu Gurugubelli
Engg., JNTU-GV College of Engineering : Professor & Head of Met

Hari Babu N
Cambridge Institute of technology : Professor and Principal

https://doi.org/10.5109/6792827

出版情報：Evergreen. 10 (2), pp.774-781, 2023-06. 九州大学グリーンテクノロジー研究教育センター
バージョン：

The Effect of ECAP on Structural Morphology and Wear Behaviour of 5083 Al Composite Reinforced with Red Mud

Brahmananda Reddy Sathi[1*], Swami Naidu Gurugubelli[2], Hari Babu N[3]

[1]Research Scholar, Department of Mechanical Engineering, JNTUK-UCE, Kakinada, AP, India-533003

[1]Deputy General Manager, Ashok Leyland, Guindy, Chennai, Tamilnadu, India-600032

[2]Professor & Head of Met. Engg., JNTU-GV College of Engineering, Vizianagaram, AP, India-535003

[3]Professor and Principal, Cambridge Institute of technology, Ranchi, Jharkhand, India- 835103

*Author to whom correspondence should be addressed:
E-mail: brahmanandareddysathi9999@gmail.com

(Received February 5, 2023; Revised April 15, 2023; accepted May 22, 2023).

Abstract: We reinforced aluminium matrix composites with three different amounts of red mud. These red mud reinforcements were manufactured using stir casting and then subjected to ECAP for evaluating the structural and wear behaviour. The formation of submicron size grains significantly enhanced the hardness, which in turn significantly lowered the loss of wear for ECAPed composites. A reduction in the wear rate was noticed with the rise in the percentage of RM reinforcement. Before ECAP, the least wear impact noted was in the composite that had 10 weight percent reinforcement. After ECAP, the least wear rate was found in the composite that had 15 weight percent reinforcement. The wear rate might have been minimized because of the elimination of the oxide layers after ECAP. At higher loads, the frictional thrust increases, consequently increasing the de-bonding and detaching of the material. Therefore, a rise in normal load raised the wear rate.

Keywords: ECAP, Aluminium matrix composites, RM reinforcement, red mud particles, molten Alloy AA 5083

1. Introduction

Primarily in energy and automobile sectors, the use of metal matrix composites of aluminium has gained worldwide attention. This is due to their ability to strengthen their monolithic counterparts. Modern technologies are currently working on enhancing conventional monolithic materials in terms of density, stiffness, and strength. Metal matrix composites are gaining significance to meet ever increasing engineering demands of severe plastic deformation techniques[1)]. Owing to their light weight, higher fracture toughness, better weight to strength ratio, etc. aluminium metal matrix composites are extensively utilized in manufacturing sectors. Hence, MMCs are finding their way into different applications such as aerospace, automotive and sports[2)].

Metal matrix composites are hybrid materials formed by blending together two or more materials whose specific attributes are imbibed in the combination[3)]. Reinforced particles are injected into a liquid matrix via liquid metallurgy to form the composite[4)-5)]. S. Basavarajappa et al, researched into the sliding wear attributes of SiC and graphite (Gr) reinforced aluminium composites and made comparisons of those with Al/SiCp reinforced Aluminum composite. They also studied the effect of wear attributes including sliding distance, normal load, etc. on the composite's dry sliding wear[6)]. C. García-Cordovilla et al., assessed several composites including AA6061/SiC, A357/SiC, AA6061/Al203, and A339/SiC in the as-cast condition for their resistance against abrasive wear[7)]. Rama Arora et al., assessed the wear attributes of an aluminium alloy (LM13), which was reinforced with 20 and 15 vwt.% TiO2 mineral of coarse (106–125 mm) and fine (50–75 mm) size ranges, at a high load swith temperature variations between 500^0C and 3000^0C[8)].

Prathipa R, et. al., worked on enhancing Hybrid Metal Matrix Composite substances by blending the appealing natures of metals and ceramics[9)]. The present study uses the Taguchi based grey relational analysis to improvize the dry sliding wear attributes of Copper (3 wt.%) and silicon carbide (5 wt.%) reinforced Aluminum LM25 matrix[10)]. Arnuri Srinivasulu et al., researched into the wear impact of T8 heat treatment on AA6063 and assessed the precipitation kinetics through XRD and SEM analysis[11)].

B.Geetha et al., analyzed the wear impact (abrasive and sliding wear) and mechanical attributes (impact strengths, compression, tensile, and micro-hardness) of composites of varied particle sizes of A356 alloy and red-mud, which are T6 heat-treated[12)]. Megumi Kawasak et al., studied high purity (99.99%), ECAP (equal-channel angular pressing) processed aluminium and accessed it with the help of orientation imaging microscopy[13]. Ananda Babu Varadala., studied the impact of casing on Al-4.5% Mg alloy, both coverless and covered with ECAE (equal channel angular extrusion) processed copper sheets. The researchers also analysed its mechanical properties and structure[14].

Priyaranjan Samal et al., carried out an investigation on attributes of RM reinforced Al-based 6082 metal matrix composites (AMMCs) using dry sliding wear mechanism[15]. Geeta B studied the impact of RM reinforced Al-6Si-0.45 Magnesium alloy (A356) on enhancing co-efficient friction, wear rate, and hardness[16]. Puri Ajay evaluated the effect of pin temperature, distance of sliding; RPM and load applied on dry sliding wear properties of RM reinforced composites of aluminium[17]. TO develop UFG materials a huge amount of strain needs to be imposed on bulk solids to acquaint with high dislocation density to rearrange an array of grain boundary. The major difficulties in the conventional working process are the lack of scope to impose a high amount of strain on the bulk solids, the variation in the size of the samples and low formability nature at lower temperatures.An attractive SPD method to develop UFG structured bulk materials is Equal Channel Angular Pressing.

Of all techniques for liquid state production, the most affordable and easiest is stir casting. When alumina is manufactured from bauxite through the Bayer's Process, the waste product produced is referred to as red mud. It is a caustic insoluble residue and comprises of alumina, titanium, silica, iron oxide, calcium oxide and trace elements (gallium and scandium).

In this paper, composites of aluminium reinforced with micron sized red mud particles synthesized by stir casting are evaluated for their mechanical attributes and wear behaviour before and after ECAP. The structural analysis is also performed by imaging via Scanning electron microscopy.

In a previous study by Rosenberger et al. (2005), the wearing of aluminium matrix composites reinforced with B2tTi, Ti3Al, B4C, and Al2O3 in quantities between 5% and 15% were investigated[18]. Another study performed by Brahmananda Reddy et al[19] conducted the DSC and TG analysis of aluminium alloy composites reinforced with red mud particle.

The proposed research work seeks to explore the effectiveness of composites of aluminium matrices reinforced with red mud. It will determine the right quantity of RM reinforcing required in the composites for attaining optimal attributes.

2. Materials and methods

2.1 Materials

AA 5083 is a matrix material and reinforcement material used is RM (red mud)[20)-25]. The chemical constitution of both AA 5083 and RM were evaluated by using optical emission spectrometer. The chemical constitution of AA 5083 is given in Table 1 and the chemical constitution of RM can be seen in Table 2, respectively. Commercially available AA5083 aluminium alloy in the form of ingots were used for stir casting purpose. RM powder of uniform size (53 microns) was used, after sieving it using mechanical sieve shaker.

Table 1. Chemical composition of AA5083

Element	**Fe**	**Mn**	**Mg**	**Cu**	**Zn**	**Si**	**Ti**	**Cr**	**Al**
%Present	0.4	0.6	4.53	0.10	0.05	0.12	00.3	0.08	Remaining

Table 2. Red mud's chemical constitution

CONSTITUENTS	**% weight (wt)**	**CONSTITUENTS**	**% weight (wt)**
Al2O3	15.0	Fe2O3	54.8
TiO2	3.7	SiO2	8.44
Na2O	4.8	CaO	2.5
P2O5	0.67	V2O5	0.38
Ga2O3	0.096	Mn	1.1
Zn	0.018	Mg	0.056
Organic C	0.88	L.O.I	Balance

2.2 Stir Casting

AA5083 ingots were cut in to pieces and placed in a crucible made with graphite kept in a stir casting furnace, maintained at a temperature of 750°C. RM powder is taken and preheated in a muffle furnace for 30 minutes at 350°c temperature, for removing the moisture content present in the RM. The pre heated RM powder is added to the molten alloy when it is being stirred at 200 rpm. Stirring is continued for 30 minutes and the alloy is poured in the mould fingers made of steel with 150 x 20 mm (height x diameter) cross sectional area. The same procedure is repeated for 5, 10 and 15 wt. % of RM particle reinforcements, and the corresponding samples are synthesized. These samples are then Equal Channel Angular Pressing (ECAP) processed shown in Fig. 2(a), (b).

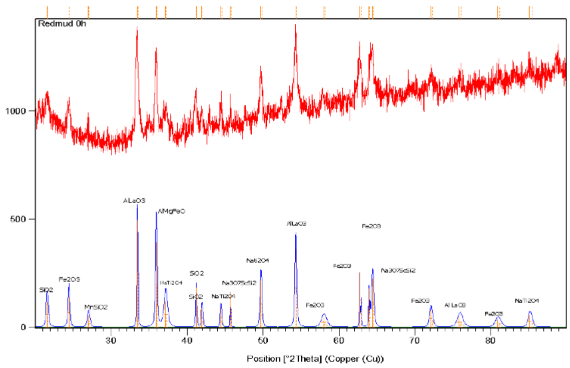

Fig. 1: X-Ray Difractogram of RM

Fig. 2: (a) Stir casting process and (b) Billets obtained after stir casting.

2.3 Equi channel angular Pressing process (ECAP)

ECAP die consists of equal channels of square section of 16mm. As seen in Fig. 3, the channels of die intersect at an outer channel angle (ψ) of 30^O and inner channel angle (φ) of 105^O.

Fig. 3: ECAP Die with a 105^O inner channel angle and 30^O outer channel angle.

The billets were annealed for 30 minutes at a temperature of 230^OC to facilitate homogenization. ECAP process was performed at room temperature using UTM. Molybdenum disulphide lubricant was coated on the samples' cross sections and the die channels to lower the friction between the samples and walls of the die. The processed samples were then taken out of the die for investigating their properties.

Hardness measurements are obtained and wear behaviour is studied. The alloy's wearing pattern is studied before and after ECAR processing.

Wear tests were performed with the help of Pin-on-wear testing machine under dry conditions in a normal laboratory setup. As seen in Fig. 4, samples from the billets were made ready in accordance with the ASTM G-99 standards. These tests were done for the composites before and after equi-channel angular processing. Tests were performed for varied loads including 10N, 20N and 30N at the speed of 200 rpm. Each test was carried out for 30 minutes and the weights of the sample prior-to and post the test was measured. By using these initial and final weights the mass loss (Δm) was calculated. A precise electronic weighing balance, which is exact up to 0.01 mg, was employed to weigh the initial and final weights. The sliding velocity and the sliding distance were calculated for each test. Care was taken that the disc and the specimens used in this process are cleaned continually with ethanol-dipped woolen fabric to prevent the adhesion of wear debris and to obtain accuracy and consistency in experimental protocols. The specimens used in the tests were fixed properly by the pin holder and the load was exerted using a dead weight hanger loading system. The frictional force generated at the rubbing surfaces are displayed on the controller. The motor's speed, which is in rpm, can be adjusted using the controller knob.

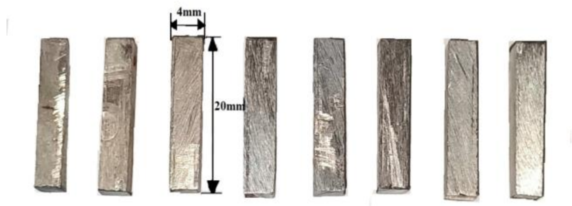

Fig. 4: Wear test samples as per ASTM G-99 standards.

The wear impact is determined from the sliding distance (L) and loss of mass by applying the formula "$W_r = \Delta m/L$". Where, Δm is the change in mass. The volumetric wear rate (Wv) of each specimen is determined by applying the density (ρ) of the specimen and the wear time (t), by applying the expression "$W_v = \Delta m/\rho t$". The specific wear impact (W_s), the wear rate due to normal force is determined by applying the formula "W_s = wear rate/ normal force". The co-efficient of friction is measured by using the equation $\mu = F_f / F_n$ in which, F_n is the load applied and F_f is the average force of friction. The specific wear rate is determined by applying the drop in the volume of the composite per unit applied normal load and per unit sliding distance to the equation- $W_s = W_v / V_s F_n$, in which V_s represents the sliding velocity.

2.4 SEM analysis

The composites' worn surfaces are evaluated by imaging them using Scanning Electron Microscopy (SEM). A variety of features, which are based on the properties of the composite, are revealed by the morphology studied through SEM.

3. Results and Discussion

3.1 Hardness Test

In this study, hardness tests are carried out with the help of Vickers hardness tester. The results prior-to and post ECAP for different samples of composites with varying fractions of RM are represented in Fig. 5. With a rise in RM, the hardness property of the composite raised up to 45% for both the alloys, before and after ECAP and the obtained results are consistent with G. Satyanarayana et al. [3]. The enhancement property is probably due to the RM particles, which fill up the voids and harden and refine the grains during the ECAP process and the formation of UFG in the reinforced material[19].

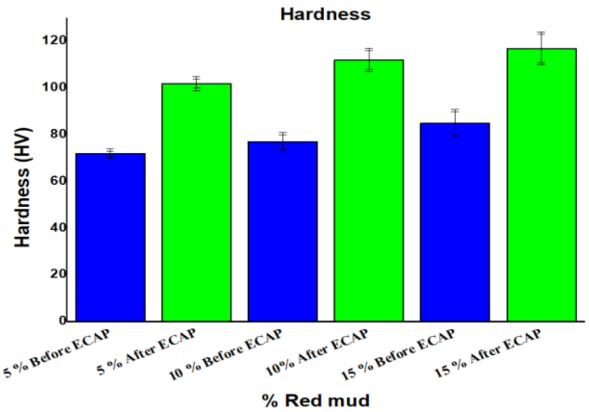

Fig. 5: Measurements of Vickers hardness before and after ECAP.

3.2 Wear Test

The 5, 10 and 15 wt. % RM particle reinforced AA 5083 composites were tested for wears both before and after equi-channel angular processing. The wear results obtained for the composites before ECAP are depicted in tables 3 to 5.

The volumetric wear (WV) and specific wear (Ws) behavior of composites with 5% wt. proportions of RM is shown in Table 3, 10% of RM shown in Table 4, and 15% of RM is shown in Table 5. The values are recorded at a constant speed of 200rpm and varying loads of 10N, 20N and 30N. The wear results obtained for the composites after ECAP are depicted in tables 6 to 8.

Table 3. AA5083+5% RM reinforcement before ECAP

Al+5% reinforcement (before ECAP) Time=1800 sec ρ=2.42 X 10^3 Kg/m^3

Load (N)	Speed (rpm)	Δm (gm)	F_f (N)	μ= (F_f/N)	Wear rate x 10^{-6} (N/m)	Volumetric wear x 10^{-12} (m^3/sec)	Specific wear x 10^{-13} (m^3/N-m)
10	200	0.097	3.3	0.33	0.8277166238	2.22681359	3.487788726
20	200	0.013	5.6	0.28	0.1109310939	2.98489378	2.337178006
30	200	0.021	7.8	0.26	0.1791963825	4.820936639	2.516960937

Table 4. AA5083+10% RM reinforcement before ECAP

Al+10% reinforcement (before ECAP) Time=1800 sec ρ=2.45 X 10^3 Kg/m^3

Load (N)	Speed (rpm)	Δm (gm)	Ff (N)	μ= (Ff/N)	Wear rate x 10^{-6} (N/m)	Volumetric wear x 10^{-12} (m3/sec)	Specific wear x 10^{-13} (m^3/N-m)
10	200	0.012	2.9	0.29	0.0102379328	2.721088435	4.261956011
20	200	0.005	5.4	0.27	0.0426658053	1.133786848	0.887907502
30	200	0.103	7.5	0.25	0.1109310939	2.747845805	1.434621749

Table 5. AA5083+15% RM reinforcement before ECAP

Al+15% reinforcement (before ECAP) Time=1800 sec ρ=2.48 X 10^3 Kg/m^3

Load (N)	Speed (rpm)	Δm (gm)	F_f (N)	μ= (F_f/N)	Wear rate x 10^{-6} (N/m)	Volumetric wear x 10^{-12} (m^3/sec)	Specific wear x 10^{-13} (m^3/N-m)
10	200	0.014	3.1	0.31	0.119464255	3.136200717	4.912133441
20	200	0.009	5.2	0.26	0.7067984496	2.016129032	1.578900034
30	200	0.010	7.2	0.24	0.853316107	2.240143369	1.169555581

Table 6. AA5083+5% RM reinforcement after ECAP

Al+10% reinforcement (after ECAP) Time=1800 sec ρ=2.45 X 10³ Kg/m³

Load (N)	Speed (rpm)	Δm (gm)	F_f (N)	μ= (F_f/N)	Wear rate x 10^{-6} (N/m)	Volumetric wear x 10^{-12} (m^3/sec)	Specific wear x 10^{-13} (m^3/N-m)
10	200	0.012	3.0	0.30	0.1023979328	2.754820936	4.314790177
20	200	0.011	5.3	0.26	0.0938647717	2.525252525	1.977612164
30	200	0.016	7.2	0.24	0.1365282514	3.673094582	1.97684523

Table 7. AA5083+10% RM reinforcement after ECAP

Al+15% reinforcement (after ECAP) Time=1800 sec ρ=2.48 X 10³ Kg/m³

Load (N)	Speed (rpm)	Δm (gm)	F_f (N)	μ= (F_f/N)	Wear rate x 10^{-6} (N/m)	Volumetric wear x 10^{-12} (m^3/sec)	Specific wear x 10^{-13} (m^3/N-m)
10	200	0.015	2.7	0.27	0.127997416	3.401360544	5.327445014
20	200	0.014	4.8	0.24	0.1194642549	3.174603174	2.486141006
30	200	0.013	6.3	0.21	0.1109310939	2.094784580	1.53903967

Table 8 AA5083+15% RM reinforcement after ECAP

Al+15% reinforcement (after ECAP) Time=1800 sec ρ=2.48 X 10³ Kg/m³

Load (N)	Speed (rpm)	Δm (gm)	F_f (N)	μ= (F_f/N)	Wear rate x 10^{-6} (N/m)	Volumetric wear x 10^{-12} (m^3/sec)	Specific wear x 10^{-13} (m^3/N-m)
10	200	0.015	2.8	0.28	0.127997416	3.360215053	50263000115
20	200	0.008	4.8	0.24	0.0682652885	1.792114695	1.403466697
30	200	0.013	6.3	0.21	0.1109310939	2.912186379	1.520422255

The corresponding graphs for the above results are drawn for specific wear rate and volumetric wear rate. The variations in specific wear rate (Ws) and volumetric wear rate (Wr) corresponding to load for 5% RM, 10% RM and 15% RM in the un-deformed condition (before ECAP). The difference in specific wear rate and volumetric wear rate corresponding to load for wear rate for 5% RM, 10% RM and 15% RM after ECAP condition. As observed, both the volumetric wear impact (Wv) and specific wear impact (Ws) decrease with a rise in load.

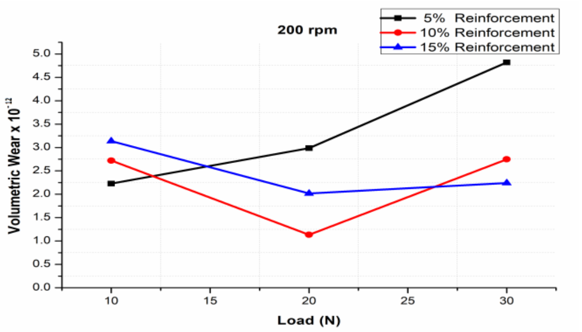

Fig. 5 Volumetric wear rate at a constant sliding speed of 200 rpm before ECAP for different % reinforcement.

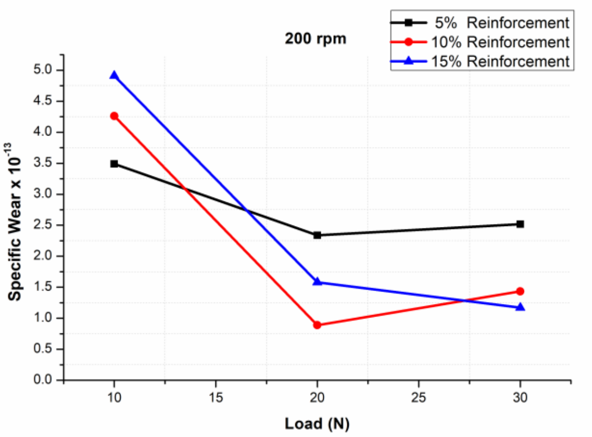

Fig. 6 Specific wear rate at a constant sliding speed of 200 rpm before ECAP for different % reinforcement.

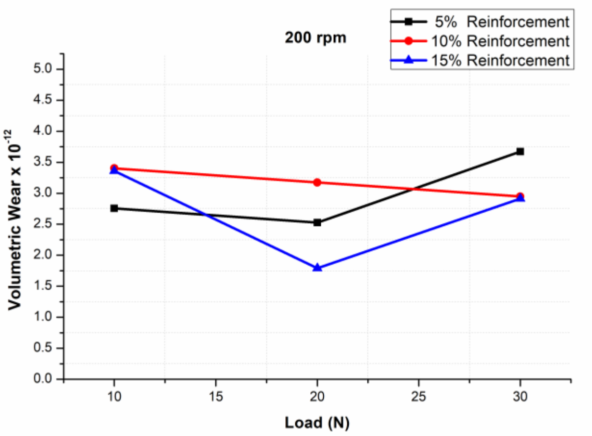

Fig. 7 Volumetric wear rate at a constant sliding speed of 200 rpm after ECAP for different % reinforcement

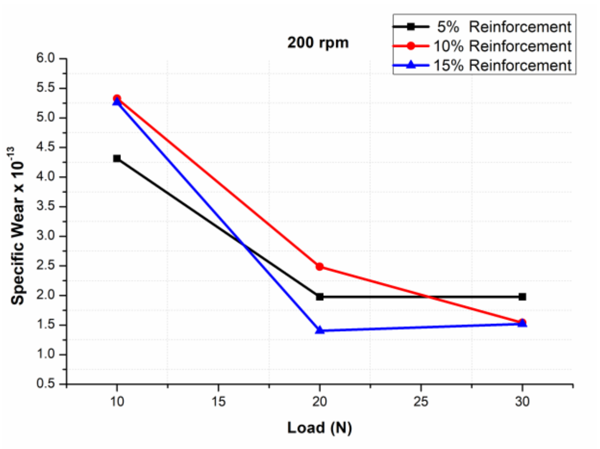

Fig.8 Specific wear rate at a constant sliding speed of 200 rpm after ECAP for different % reinforcement

The slightest wear impact is seen at 20 N, and beyond 20 N there is an ascent in the wear rate. The composite in the un-deformed condition with 10 wt.% RM reinforcement has shown the least wear rate at this load. After ECAP, the composite with 15 wt% RM reinforcement has shown the least wear rate. As observed, initially, the specific wear is higher owing to the due to extra strokes between the steel disc and the pin surface. A gradual reduction in specific wear with increasing sliding distance was observed for all types of billets. This is experienced due to strain hardening[26].

3.3 Scanning Electron Microscopy

SEM micrographs of worn out planes of composites obtained before ECAP is shown in Fig. 9 and after ECAP is shown in Fig. 10 at varied loads and at a constant sliding velocity of 200 rpm. The worn SEM images of 5% RM reinforced composite worn surfaces at varied loads viz., 10N, 20N and 30N are given in Fig. 9(a), Fig. 9(b) and Fig.9(c). The worn SEM images of 10% RM reinforced composite worn surfaces at varied loads viz., 10N, 20N and 30N are seen in Fig. 9(d), Fig. 9(e) and Fig. 9(f). The worn SEM images of 15% RM reinforced composite worn surfaces at varied loads viz., 10N, 20N and 30N are given in Fig.9 (g), (h) and (i).

The worn surfaces show wear debris, de-lamination and ploughing owing to the emergence of subsurface cracks. This caused the shedding off of composite material that took forms like wear debris or flakes[27)-30)]. The cracks on the surfaces of the samples nucleated at higher loads. This was due to the action of tangential forces between the surfaces in contact[31)].

These cracks are propagated along the wear track and caused de-lamination that resulted in the rupture of debris and development of craters. When the planes of the pin and disc rubbed against each other, some substance from the pin's plane got detached, taking the shapes of tiny fragments and ploughing wear. The detachment of wear debris during de-lamination causes the formation of craters in the worn surfaces. The production of oxide layers on the composite with 10 wt% RM were lower, and hence, possessed higher wear resistance.

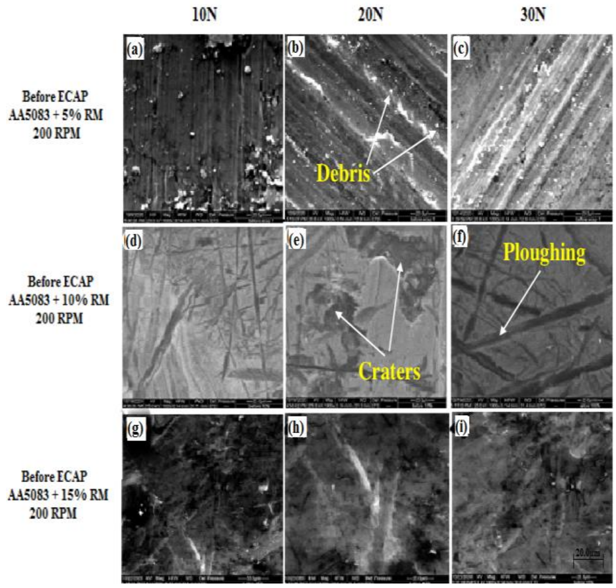

Fig. 9: SEM micrographs of worn out planes before ECAP

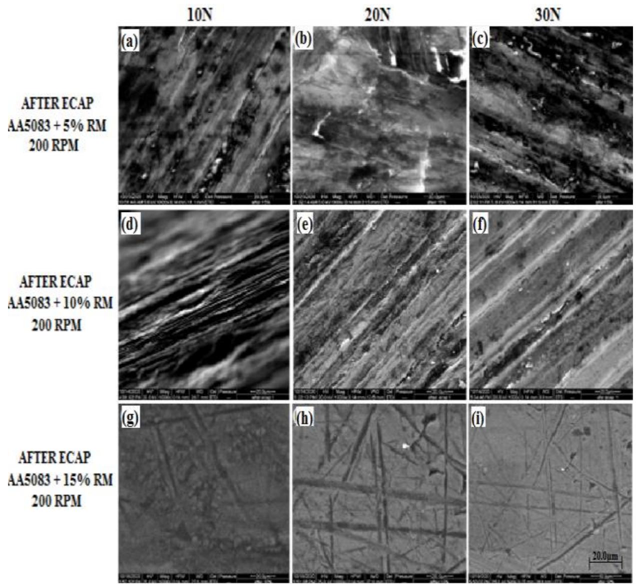

Fig. 10: The detailed SEM micrographs of worn out planes after ECAP.

4. Conclusions

The below-given conclusions are derived from the investigations carried out in this research.

The formation of UFGs in the severely deformed Al-red mud composites lowered the wear rate considerably for all the weight proportions of reinforcements. Nano-structured red mud reinforcement composites had shown increased wear rate for deformations after 20% because of softening of strain.

The frictional thrust increases at larger loads, resulting in a rise in de-bonding and detaching of material. Therefore, with a rise in normal load, the wear rate also increases. In all cases, the friction coefficient reduced with a rise in normal force. This is due to the matrix wear from the surface of the pin, which rounds off the particulates.

An increase in reinforcement percentage leads to a diminish in the wear rate. Before ECAP, least wear rate noticed was in the 10 wt. % reinforced composite. After ECAP, the least wear rate noticed was in the 15 wt % red mud reinforced composite. The elimination of oxide layers post ECAP may be the causative factor of the minimized wear rate.

References

1) Callister William D Jr., 2007, "Materials Science and Engineering- an introduction", 7th edition, John *Wiley & Sons. Inc*.– NewYork, USA.
2) HanBQ and LangdonTG, *Mater Sci Eng* A410 (2005) 430.
3) G. Satyanarayana; G. Swami Naidu; N. Hari Babu, "The effect of deformation on wear behaviour of Al-5% red mud particle reinforced nano composites synthesised by stir casting", *Int. J. of Materials Engineering Innovation*, Inderscience Publishers, 2016 Vol.7, No.2, pp.115 - 129
4) Koczak, M.J. and Prem Kumar, M.K. (1993) "Emerging technologies for the in-situ production of MMCs", *JOM*, Vol. 45, No. 1, pp.44–48.
5) Hashim, J., L. Looney, M.S.J. Hashmi, 1999. "Metal matrix composites: production by the stir casting method", *Journal of materials processing technology, Elsevier B.V., Netherlands,* Volume92-93, pp. 1-7.
6) Basavarajappa S, Chandramohan G, Davim J Paulo. "Application of Taguchi techniques to study dry sliding wear behaviour of metal matrix composites" *Materials and Design* 2007; 28:1393–1398
7) Garcia-Cordovilla C, Narciso J, Louis E. "Abrasive wear resistance of aluminium alloy /ceramic particulate composites" *Wear*, 1996; 192:170-177
8) Arora Rama, Kumar Suresh, Singh Gurmel, Pandey OP. "Influence of particle size and temperature on the wear properties of rutile-reinforced aluminium metal matrix composite", *Journal of Composite Materials,* 2015; 49 :843–852
9) Prathipa, R. "Mechanical Characteristics Of Aluminium 5083 Metal Matrix Strengthen With Fly Ash." *Turkish Journal of Computer and Mathematics Education (TURCOMAT)* 12.10 (2021): 2153-2164.
10) Muthu, Poovalingam. "Multi objective optimization of wear behaviour of Aluminum MMCs using Grey-Taguchi method." Manufacturing Review 7 (2020): 16.
11) Arnuri, Srinivasulu, and Swami Naidu Gurugubelli. "The Effect of T8 Heat Treatment on Wear Behaviour and Microstructure of 6063 Aluminium Alloy Deformed by Cryo and RT ECAP." *Forming the Future. Springer, Cham*, 2021. 1727-1741.
12) Geetha, B., and K. Ganesan. "Experimental investigation on influence of particle size on mechanical properties and wear behaviour of A356-red mud metal matrix composite." *AIP Conference Proceedings.* Vol. 2128. No. 1. AIP Publishing LLC, 2019.
13) Kawasaki, Megumi, Zenji Horita, and Terence G. Langdon. "Microstructural evolution in high purity aluminum processed by ECAP." *Materials Science and Engineering:* A 524.1-2 (2009): 143-150.
14) Ananda Babu Varadala, Swami Naidu Gurugubelli, Sateesh Bandaru, "Enhancement of structural and mechanical behavior of Al-Mg alloy processed by ECAE", *Materials Today: Proceedings,* Volume 18, Part 6, 2019, Pages 2147-2151, ISSN 2214-7853,
15) Samal, Priyaranjan, Ravi Kumar Mandava, and Pandu R. Vundavilli. "Dry sliding wear behavior of Al 6082 metal matrix composites reinforced with red mud particles." *SN Applied Sciences* 2.2 (2020): 1-11.
16) Geetha, B., and K. Ganesan. "Effects of Red Mud Reinforcement on Hardness, Wear Behaviour of Cast Al-6Si-0.45 Mg Alloy", *Applied Mechanics and Materials.* Vol. 787. Trans Tech Publications Ltd, 2015.
17) Puri Ajay, J., and S. A. Sonawane. "Experimental Investigation of Wear Properties of Aluminium LM25 Red Mud Metal Matrix Composite." *International journal for scientific research & development* 3 (2015): 691-6
18) Rosenberger, M.R., Schvezov, C.E. and Forlerer, E. (2005) "Wear of different aluminium matrix composites under conditions that generate a mechanically mixed layer", *Wear,* July–August, Vol. 259, Nos. 1–6, pp.590–601.
19) Brahmananda Reddy Sathi, Swami Naidu Gurugubelli, Hari Babu(2019) "TG and DSC Analysis of Equi-Channel Angular Processed Red Mud Particle Reinforced 5083 Aluminium Alloy Matrix Composites Synthesized by Stir Casting" *Transactions of the Indian Institute of Metals*, 73, 1655–1659 (2020)
20) Grujicic M, Arakere G, Pandurangan B, Hariharan A, Yen CF, Cheeseman B A, and Fountzoulas C, *J Mater Eng Perform* 20 (2011) 855.
21) Valiev R Z, and Langdon T G, Prog Mater Sci 51 (2006) 881. Langdon T G, *Mater Sci Eng* A462 (2007) 3
22) P. K. Rohatgi, B. F. Schultz, A. Daoud, and W. W. Zhang, "Tribological performance of A206 aluminum alloy containing silica sand particles," *Tribology International*,vol. 43, no. 1-2, pp.
23) A. Mahyudin, S. Arief, H.Abral, M. Muldarisnu, M.P. Artika, "Mechanical Properties and Biodegradability of Areca Nut Fiber-reinforced Polymer Blend Composites," *Evergreen*, 7(3), 366-372 (2020). https://doi.org/10.5109/4068618
24) H. Sosiati, Y.A. Shofie, A.W. Nugroho, "Tensile properties of Kenaf/E-glass reinforced hybrid polypropylene (PP) composites with different fiber loading," *Evergreen,* 5(2), 1-5 (2018).

https://doi.org/10.5109/1936210

25) A. Kumar, A.K. Chanda, S. Angra, "Optimization of Stiffness Properties of Composite Sandwich using Hybrid Taguchi-GRA-PCA," *Evergreen*, 8(2), 310-317 (2021). https://doi.org/10.5109/4480708
26) G. A. Edwards, K. Stiller, G. L. Dunlop, and M. J. Couper, *Acta Mater*, 46 (1998) 3893.
27) I. Sabirov, O. Kolednik, R. Z. Valiev, and R. Pippan, *Acta Mater* 53 (2005) 4919.
28) F. D. Dumitru, O. F. Higuera-Cobos, and J. M. Cabrera, *Mat Sci Eng* A, 594 (2014) 32.
29) K. Sivaprasad, S. P. K. Babu, S. Natarajan, R. Narayanasamy, B. A. Kumar, and G. Dinesh, *Mat Sci Eng A* 498 (2008) 495.
30) Harini Sosiati, Yankeisna Auda Shofie and Aris Widyo Nugroho, Tensile Properties of Kenaf/E-glass Reinforced Hybrid Polypropylene (PP) Composites with Different Fiber Loading, *EVERGREEN Joint Journal of Novel Carbon Resource Sciences & Green Asia Strategy*, 5(2), 1-5 (2018). https://doi.org/10.5109/1936210
31) H. Sosiati, Y. A. Shofie and A. W. Nugroho, "Tensile Properties of Kenaf/E-glass Reinforced Hybrid Polypropylene (PP) Composites with Different Fiber Loading". *EVERGREEN Joint Journal of Novel Carbon Resource Sciences & Green Asia Strategy*, 5(2), 1-5 (2018). https://doi.org/10.5109/1936210